https://doi.org/10.5194/wes-2026-218
Preprint. Discussion started: 24 November 2026
© Author(s) 2026. CC BY 4.0 License.

eawe european academy of wind energy
Open Access WIND ENERGY SCIENCE DISCUSSIONS

The IEA Reference Hybrid Power Plant

Jenna Iori[1], Katarina Obradovic[2], Matteo Baricchio[3], Jared J. Thomas[4], Megha Gupta[2], Ralph Bou Ghanem[5], Antonio Notholt[6], Daniel Pombo[7], Christopher Bay[4], and Kaushik Das[2]

[1]Faculty of Aerospace Engineering, Delft University of Technology, Delft, The Netherlands
[2]Department of Wind and Energy Systems, Technical University of Denmark, Roskilde, Denmark
[3]Faculty of Mechanical Engineering, Delft University of Technology, Delft, The Netherlands
[4]National Laboratory of the Rockies, Golden CO, United States
[5]Solar Lab, ENGIE Laborelec, Linkebeek, Belgium
[6]School of Engineering, Reutlingen University, Reutilingen, Germany
[7]EPRI Europe, Nexus UCD, Belfield Office Park, Beech Hill Road, Dublin, D04 V2N9, Ireland

Correspondence: Jenna Iori (j.iori@tudelft.nl)

Abstract.

This article presents a reference design for a hybrid power plant consisting of a wind farm, solar photovoltaics (PV) farm, and battery energy storage system. The power plant is designed for an onshore site in western Denmark and for a limited grid connection capacity of 300 MW. The wind farm is made of 65 NLR 5 MW reference turbines, for a total capacity of 325 MW, placed in a grid layout. The solar PV farm consists of 59 modular solar PV systems with a total capacity of 400 MWp and an AC/DC ratio of 1. The storage system has a power capacity of 150 MW and an energy capacity of 300 MWh, divided into 60 lithium-ion battery units. We present an example simulation of the design and associated performance metrics. The novelty of this dataset resides in the high level of detail in the specification of each of the components, thereby enabling advanced simulation studies and supporting research and development efforts for hybrid power plants.

Nomenclature

AEP - annual energy production
CAPEX - capital expenditures
EMS - energy management system
GHI - global horizontal irradiance
HPP - hybrid power plant
IEA - International Energy Agency
IRR - internal rate of return
LCOE - levelized cost of energy
NPV - net present value
OPEX - operational expenditures
PV - photovoltaic

https://doi.org/10.5194/wes-2026-218
Preprint. Discussion started: 24 November 2026
© Author(s) 2026. CC BY 4.0 License.



eawe european academy of wind energy
Open Access WIND ENERGY SCIENCE DISCUSSIONS

TCP - Technology Collaboration Programme

1 Introduction

Broadly speaking, a hybrid power plant (HPP) can be defined as "a combination of two or more independent electricity generation and/or storage technologies providing coordinated electrical power services that are connected at a single point" (IEA Wind Technology Collaboration Programme, n.d.). By sharing electrical infrastructure such as transformers, substations, and grid interconnection, HPPs hold the potential to reduce balance-of-system costs while improving resource utilization, curtailment management, and market responsiveness (Das et al., 2025). Following the global interest in solar, wind, and battery energy storage systems, both in academia (Valencia Ochoa et al., 2019) and practice (International Energy Agency, 2020), the focus of this work is on those three technologies combined in a utility-scale, grid-connected, co-located onshore power plant.

Existing utility-scale onshore HPP research covers a wide range of design-related problems, showing sustained interest in better understanding and developing HPPs. Design-related problems include sizing (where the goal is to identify optimal configurations that maximize energy output, minimize costs, enhance value, improve financial performance, or increase reliability across different combinations of wind, solar, and storage), operations (such as the design of energy management systems and control coordination of technologies), and physical design (layout planning and electrical infrastructure design). Multiple studies consistently highlight both the significant promise of HPPs and the need for continued research advances (Veers et al., 2022; WindEurope, 2019; Dykes et al., 2020; Das et al., 2025; Obradović et al., 2025; O'Malley et al., 2024).

Most HPP design studies validate their approaches using site-specific cases tailored to local conditions. Variations in plant capacity, technology mix, network topology, and regulatory requirements make it difficult to directly compare proposed methods or to relate them to a common industry baseline. With the expectation that research will expand further, creating a single reference point can streamline advances in the state-of-the-art HPP design, thus supporting their faster real-world implementation.

Reference designs, in this context, offer one design solution which can serve as a fixed starting point for further research and comparison. In the present work, a *reference design* is meant to provide an example of a detailed design, not the best possible design, as the definition of "best" can vary based on the objective and constraints. The proposed design, in its full scope or in part (depending on the application), can serve as a benchmark for different optimization frameworks, technical ideas for design improvements and their comparison against multiple key performance indicators.

Unlike industry guidelines from financial organizations (e.g., International Finance Corporation, World Bank, European Investment Bank), which typically outline principles or best practices, reference designs define a single, fully specified configuration. In contrast to many industry standards, which often address only specific subsystems and may be mandatory, a reference design proposes an integrated, end-to-end plant solution aligned with such relevant standards. It enables consistent benchmarking of new methods, optimization frameworks, and control strategies against a shared, feasible baseline.

https://doi.org/10.5194/wes-2026-218
Preprint. Discussion started: 24 November 2026
© Author(s) 2026. CC BY 4.0 License.



eawe european academy of wind energy
Open Access WIND ENERGY SCIENCE DISCUSSIONS

Reference designs have already proven valuable in renewable energy research, including applications to wind turbines (Zahle et al., 2024) and offshore wind farms (Hall et al., 2024; Kainz et al., 2024). For hybrid systems combining renewable and non-renewable technologies, an open reference platform for integrated energy systems was proposed several years ago (Svendsen et al., 2023). Similarly, in power system analysis, standardized test networks from IEEE and CIGRE have been the common practice for effective comparison for many years (Peyghami et al., 2019).

1.1 Limitations and challenges

Defining a reference design for renewable HPPs presents unique challenges compared to single-technology power plants like wind farms. First, the boundaries of the HPP design problem are weakly defined. A variety of key performance indicators, such as levelized cost of energy (LCOE), net present value (NPV), internal rate of return (IRR), and grid utilization factor, can be used. Problem constraints are often applied corresponding to the specific components of the power plant, but there are none that are specific to HPPs as a whole. The lack of a standardized design problem means that a reference design lacks universal applicability. This work does not propose a globally optimized HPP design solution or a novel design methodology, but it can be a starting point for developing one.

The second challenge is the modularity of HPPs. The type of components in a given HPP and the dimension can be chosen to optimize a given performance metric but will vary with a change of objective. Thus, the lack of strict design constraints results in a large variety of feasible designs and raises the question of which method to use to select the "best" design.

A third challenge comes from the site-specificity of this type of power plant. Different design problems in HPPs are often informed by electricity price data and site conditions, e.g., wind and solar resource data and their correlation. A standardized classification system for site resources for HPP has yet to be developed. As a result, an HPP design is tied to the specific location and associated bidding zone corresponding to the input data.

All these challenges point towards an ambiguity in the definition of a reference design when applied to HPPs. To provide a starting point and support system integration studies in wind and solar energy, we present the detailed specification of a reference HPP design, which can, to varying degrees, be used for different design sub-problems, including sizing, energy management, and physical design, among others. As mentioned, the proposed power plant design is made of a combination of a wind farm, a solar PV farm, and a battery energy storage system, corresponding to an onshore location in Denmark.

The remainder of the article is organized as follows. Section 2 reports the general characteristics of the reference HPP design and details the design process. Section 3 provides a detailed description of the major components of the HPP: the wind farm, the solar PV farm, the battery energy storage system, and the shared electrical infrastructure. Section 4 reports the performance of the power plant for an example simulation, and Section 7 concludes the article. This effort is the result of Work Package 2 of the International Energy Agency Wind Technology Collaboration Programme (IEA Wind TCP) Task 50[1], an international collaborative effort aiming to coordinate global research and development in the field of HPPs.

[1] https://iea-wind.org/task50/

https://doi.org/10.5194/wes-2026-218
Preprint. Discussion started: 24 November 2026
© Author(s) 2026. CC BY 4.0 License.



eawe european academy of wind energy
Open Access WIND ENERGY SCIENCE DISCUSSIONS

2 Hybrid power plant design

In this section, the general characteristics of the reference HPP design are reported. Due to the complexity and multidisciplinary nature of the design problem, the design process was divided into several steps, explained in Section 2.1. We then describe the site chosen for the design (Section 2.2) and the system-level properties of the power plant (Section 2.3).

2.1 Design process

The design process of the reference HPP was conducted in several steps, namely (i) definition of the boundaries of the problem, (ii) generation of the optimal system-level parameters of the plant, and (iii) generation of the detailed design of the power plant components.

The problem boundaries are chosen to represent a common use case for the deployment of HPPs. We consider an onshore grid-connected HPP with a fixed grid capacity of 300 MW, reflecting realistic transmission capacity constraints in high-renewable regions. The goal of the design process is to make the best use of the limited grid connection, including considering revenue from the electricity market, capital expenditures (CAPEX), and curtailment. We consider three commonly used technologies for the components of the power plant: a wind farm, a solar PV farm, and a lithium-ion battery energy storage system. All three subsystems are co-located behind the same shared connection point, enabling infrastructure cost sharing and coordinated operation through a centralized energy management system. Denmark is selected for the location of the site due to its strong wind potential, increasing solar deployment, mature electricity markets, and well-established grid infrastructure, making it a representative case for large-scale hybrid energy systems. The site is described further in Section 2.2.

With these problem boundaries, the system-level properties of the power plant are generated by solving an optimization problem with the open-source framework HyDesign (Murcia Leon et al., 2024). HyDesign integrates plant sizing and operational optimization to identify the economically optimal hybrid configuration considering the problem boundaries. The system-level properties of the design are reported in detail in Section 2.3.

The design of each component of the power plant is then detailed further using the system-level properties as an input. This step is necessary because design frameworks such as HyDesign typically use simplified models and parametrizations for the power plant components in order to make the optimization problem tractable. The wind farm layout is generated by solving an integrated design optimization problem with the H2Integrate software (Brunik et al., 2025). The characteristics of the solar PV farm and modules, battery and electrical infrastructure are decided by subject matter experts from both industry and academia participating in the IEA Wind TCP Task 50. The detailed design for each component and the associated design methodologies are reported in Section 3.

2.2 Site characteristics

The site chosen for the design is located in the central part of the Jutland region in Denmark, with coordinates 56.22°N, 8.59°E (see Fig. 1). We assume that there is sufficient available space at this location for the installation of the power plant. Constraints

https://doi.org/10.5194/wes-2026-218
Preprint. Discussion started: 24 November 2026
© Author(s) 2026. CC BY 4.0 License.



eawe european academy of wind energy
Open Access WIND ENERGY SCIENCE DISCUSSIONS



Figure 1. Site location. (Sources: Esri, TomTom, Garmin, FAO, NOAA, USGS, © OpenStreetMap contributors, and the GIS User Community. Licensed under the ESRI Master License Agreement.)

associated with residential or protected areas are not considered. Furthermore, the effect of vegetation and topography are neglected.

The solar and wind resource assessments are based on high-resolution meteorological time series obtained from the Open-Meteo API and the ERA5 reanalysis dataset (Zippenfenig, 2023; Hersbach et al., 2023). The same source is used for both resources to ensure internal consistency across technologies. The dataset corresponds to the site location and provides hourly temporal resolution for the meteorological and radiative variables over the period 2002–2022.

The irradiance at the site location yields an average annual global horizontal irradiance (GHI) of 1,095 kWh·m^{-2}, corresponding to a mean daily GHI of 3.0 kWh·m^{-2}. The distribution of GHI is illustrated in Fig. 2. This corresponds to a moderate solar resource, typical of northern European locations. The dataset further provides separate components of direct normal irradiance and diffuse horizontal irradiance, enabling a physically consistent representation of irradiance conditions and supporting subsequent transposition to the plane of array for PV performance modelling.

This site is associated with relatively good wind resource with a mean wind speed of 8 m·s^{-1} at a hub height of 90 m, with a dominant northwesterly direction. The wind speed data at hub height is scaled from the available 100 m data using a wind shear $\alpha = 0.14$. This value is obtained by fitting a power law to the wind speed data at 10 m and 100 m over the 20-year period over all wind directions. The sectoral Weibull distributions are reported in Table 1. Figures 3 and 4 illustrate the wind speed and wind direction distributions for the dominant direction sector. Finally, we observe a negative correlation at this location between the wind and solar resource, as reported in Fig. 5.

2.3 System-level properties

The dimensions and characteristics of the power plant components are generated by solving a design optimization problem with the open-source tool HyDesign (Murcia Leon et al., 2024). The objective of the problem is to maximize the net present

https://doi.org/10.5194/wes-2026-218
Preprint. Discussion started: 24 November 2026
© Author(s) 2026. CC BY 4.0 License.

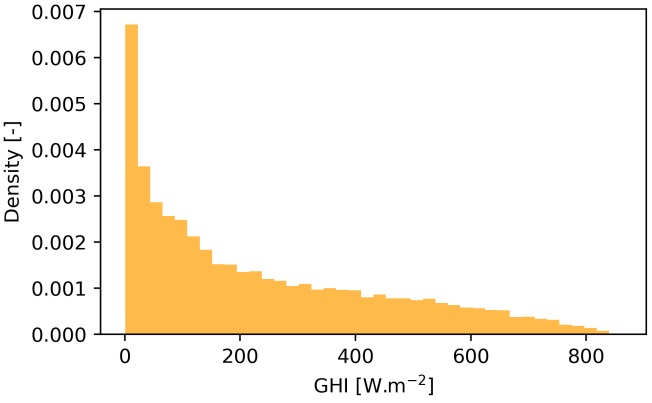

Figure 2. Distribution of the hourly global horizontal irradiance (GHI) at the site location for the period 2002 to 2022.

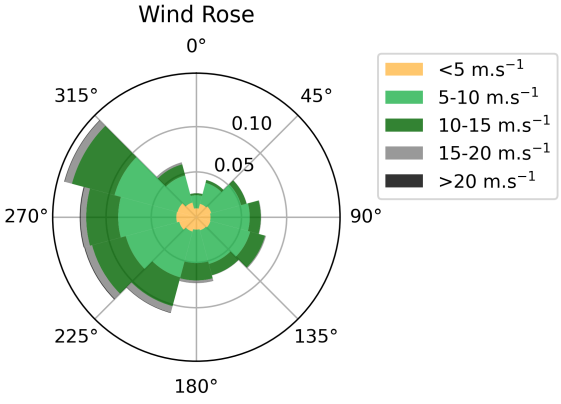

Figure 3. Distribution of wind speed and wind direction at hub height, for wind direction bins of 30°.

value over capital expenditure (NPV/CAPEX), accounting for the relative profitability and capital efficiency of the project, and enabling a fair comparison between alternative plant designs with different investment sizes.

The HPP sizing problem is formulated as a nested optimization problem. The outer optimization layer determines the optimal capacities and key design parameters of the power plant: number of wind turbines, wind turbine specific power, rated power and height clearance, wind farm installation density, solar PV farm capacity, solar PV module orientation, solar PV AC/DC ratio, and battery sizing in terms of duration and power capacity. For the wind farm power production, we use a generic farm layout with a circular boundary and regular turbine spacing. The wake losses are modelled with a Gaussian wind speed wake deficit, implemented in PyWake (Pedersen et al., 2023). The wind turbines are represented by a generic wind turbine power curve. The solar PV farm power production is calculated based on a generic plant configuration and models implemented in PVLib (Anderson et al., 2023). The use of simplified models allows the optimization problem to be tractable while exploring the design space efficiently. The inner optimization layer represents the energy management system (EMS) and determines the

https://doi.org/10.5194/wes-2026-218
Preprint. Discussion started: 24 November 2026
© Author(s) 2026. CC BY 4.0 License.

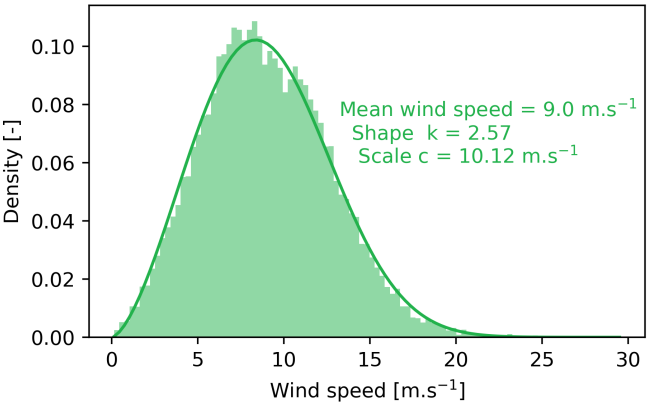

Figure 4. Distribution of the hourly wind speed at hub height and for the wind direction sector centered around 300° at the site location for the period 2002 to 2022, and corresponding fitted Weibull distribution.

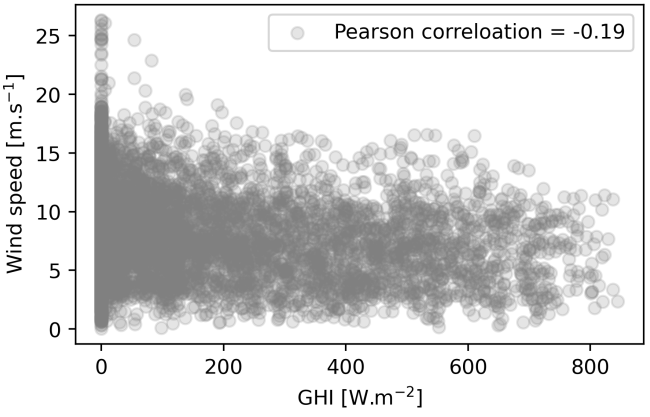

Figure 5. Correlation between wind speed and irradiance for the year 2022.

optimal dispatch, curtailment, storage usage, and electricity export strategies to maximize revenues from the spot market while accounting for battery degradation and operational constraints.

The outer sizing problem is a non-linear program and is solved using a parallel efficient global optimization algorithm, which is a surrogate-based method designed to minimize the number of expensive model evaluations while ensuring global optimality. The inner optimization problem is formulated as a linear problem and solved with the off-the-shelf solver CPLEX (IBM, 2024). We refer the reader to the article by Murcia Leon et al. (2024) for more details on the optimization problem and its implementation.

The system-level parameters of the reference design obtained with this methodology are listed in Table 2. With this preliminary analysis, the wind farm is made of 65 turbines, each with 5 MW capacity, rotor diameter of 161.5 m and hub height of

https://doi.org/10.5194/wes-2026-218
Preprint. Discussion started: 24 November 2026
© Author(s) 2026. CC BY 4.0 License.



eawe european academy of wind energy
Open Access WIND ENERGY SCIENCE DISCUSSIONS

Table 1. Weibull distribution of the wind speed at hub height per wind direction bins and frequency of occurrence.

Bin center [^{o}]	Shape [-]	Scale [m.s$^-$1]	Frequency
0	2.28	6.91	2.7 %
30	2.36	6.84	4.3 %
60	2.48	7.48	5.8 %
90	2.66	8.19	7.2 %
120	2.66	8.60	8.0 %
150	2.68	8.33	6.7 %
180	2.40	9.31	7.3 %
210	2.48	10.12	11.0 %
240	2.46	10.12	12.9 %
270	2.38	9.73	12.9 %
300	2.57	10.12	15.2 %
330	2.18	8.56	6.3 %

140.8 m. The wind farm uses an area of 46.4 km^2, corresponding to a power density of 7 MW·km^{-2}. The solar PV system has an AC/DC ratio of 1 and occupies an area of 4.9 km^2, with modules installed at a 25° tilt angle and 180° azimuth. Due to degradation, the battery needs to be replaced twice over the project lifetime.

Table 2. System-level parameters of the reference design, in absolute value and relative to the grid connection capacity.

	Capacity	Value relative to the grid connection
Wind farm	325 MW	1.08
Solar PV	400 MW	1.33
Battery	150 MW / 300 MWh	0.5 / 1h
Grid connection	300 MW	-

3 Power plant components design

Based on the system-level parameters of the power plant, the design of each component of the HPP is defined with a higher level of detail as described in the following sections: wind farm design and layout (Section 3.1), solar PV module and farm (Section 3.2), energy storage system (Section 3.3) and electrical infrastructure (Section 3.4).

3.1 Wind farm

The wind farm was designed using the National Laboratory of the Rockies' (NLR's) holistic hybrid integration (H2Integrate) software (Brunik et al., 2025) because it allows for wind farm layout optimization, including wind turbine wake effects and

https://doi.org/10.5194/wes-2026-218
Preprint. Discussion started: 24 November 2026
© Author(s) 2026. CC BY 4.0 License.



eawe european academy of wind energy
Open Access WIND ENERGY SCIENCE DISCUSSIONS

the full hybrid plant model in the optimization model. H2Integrate allows users to bring together a range of tools and models for specific subsystems and combines them into a larger hybrid system model. While some hybrid system models rely on simplistic, often linearized, models of the subsystems, the modular and extensible design of H2Integrate allows for detailed discipline-specific models that have been developed independently to be easily combined and executed together to model the operation of a full hybrid system. Thus, H2Integrate allows for subsystem design (e.g. wind farm layout), while accounting for the combined influence of other subsystems in the plant (e.g. solar PV electricity generation) on the objective function (e.g. LCOE of the full HPP). To design the wind farm layout, we also modelled the rest of the hybrid system so that the wind farm design would take into account the impact of the solar PV and battery system performance on the overall HPP cost and performance characteristics.

The wind farm was modelled within H2Integrate using Ard (Frontin et al., 2024). Ard brings together various wind farm and wind turbine models (including the Wind-plant Integrated System Design and Engineering Model (WISDEM v4.1.0) for wind farm cost estimation (National Laboratory of the Rockies (NLR), 2026b), FLORIS v4.3 for wind farm aerodynamic modelling and energy estimation (National Laboratory of the Rockies (NLR), 2026a), and OptiWindNet for wind farm electrical cable array design (Souza de Alencar et al., 2026)) into a single wind farm modelling and design tool to handle costs, aerodynamics, and turbine and cable layout within a single analysis framework. Within FLORIS, we used a Gaussian wake model and other default modelling parameters. The solar PV performance was modelled using PVWatts v8 algorithm from PySAM (National Laboratory of the Rockies (NLR), 2025). The battery was modelled using a simple generic storage model from H2Integrate, which uses a heuristic approach based on charge/discharge rates, capacity, max/min state of charge, and efficiencies to model battery performance with a target demand profile. We obtained our LCOE estimation by solving for the break-even price in a cash flow analysis of the hybrid system. The cash flow analysis was performed within H2Integrate using ProFAST (Kee and Penev, 2023), a Python implementation of H2FAST (Penev et al., 2019), which performs a cash-flow system analysis using generally accepted accounting principles. Both Ard and H2Integrate are built on NASA's open-source multidisciplinary analysis and optimization software, OpenMDAO (Gray et al., 2019).

The wind resource is described by the time series of wind speed and wind direction for the year 2022. We assumed a constant turbulence intensity of 0.1 for all wind conditions. To simplify the design process, we also assumed an 46.4 km^2 area was available for wind turbine placement and that turbines would be placed in rows and columns in a uniform grid, but that column and row spacing was variable, as was the grid orientation and skew angle (see Stanley and Ning (2019) for more information). We also enforced a minimum turbine spacing of 0.552 km (4.37 rotor diameters) between wind turbines. The rest of the inputs for the wind farm design are chosen to match the system-level parameters of the HPP. We used the NLR 5 MW reference turbine (Jonkman et al., 2009) in the design because it had the desired rating and detailed open-source information available. Additional modelling assumptions and results are provided in Table A1.

An optimization problem is formulated to obtain the optimal wind farm layout, defined by the positions of the wind turbines $(\boldsymbol{x}, \boldsymbol{y})$ and the substation $(x_{\text{sub}}, y_{\text{sub}})$. To reduce the dimensionality of the problem, the wind layout is parametrized using four different variables, namely, primary spacing Δx, secondary spacing Δy, orientation angle α, and skew angle β, resulting in a

https://doi.org/10.5194/wes-2026-218
Preprint. Discussion started: 24 November 2026
© Author(s) 2026. CC BY 4.0 License.



eawe european academy of wind energy
Open Access WIND ENERGY SCIENCE DISCUSSIONS

200 grid layout. This definition follows the implementation of a grid layout in Ard, as illustrated in Fig. 6, which is based on the work of Stanley and Ning (2019).

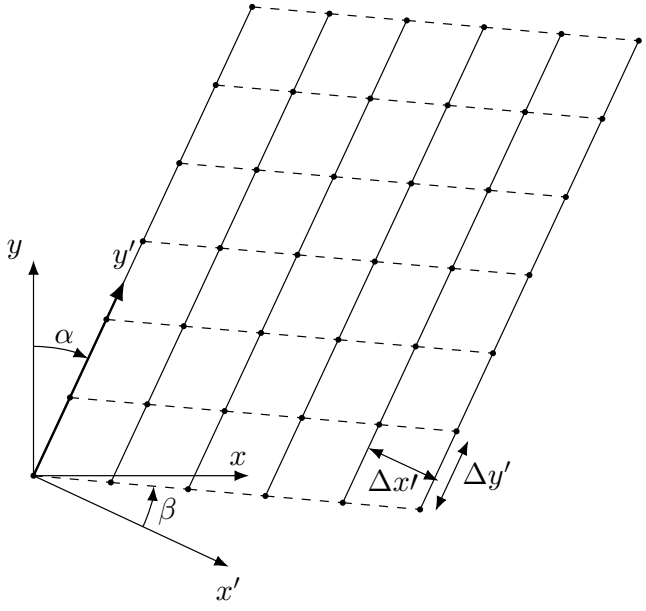

Figure 6. Grid layout definition used in Ard. The wind farm grid is rotated into the (x', y') coordinate frame from the primary coordinate frame (x, y) by the orientation angle α. The grid is skewed away from a regular grid by the skew angle, β. Turbines are separated along the y' direction by the primary spacing, $\Delta y'$. Turbines are separated along the x' direction by the secondary spacing, $\Delta x'$, with the secondary spacing being perpendicular to the primary spacing.

The optimization problem is formulated as:

$$
\begin{aligned}
\min_{\substack{x_{\text{sub}}, y_{\text{sub}} \\ \Delta x, \Delta y, \alpha, \beta}} \quad & \text{LCOE}(x_{\text{sub}}, y_{\text{sub}}, \Delta x, \Delta y, \alpha, \beta) \\
\text{subject to} \quad & (\boldsymbol{x}, \boldsymbol{y}) \in A \\
& \sqrt{(x_i - x_j)^2 + (y_i - y_j)^2} \geq 552\,\text{m} \quad \forall i, j \in [1, N_{wt}],\ i \neq j \\
& x_{\text{sub}} \in [-3405.9\,\text{m}, 3405.9\,\text{m}] \\
& y_{\text{sub}} \in [-3405.9\,\text{m}, 3405.9\,\text{m}] \\
& \Delta x' \in [3\,D, 20\,D] \\
& \Delta y' \in [3\,D, 20\,D] \\
& \alpha \in [-180^\circ, 180^\circ] \\
& \beta \in [-75^\circ, 180^\circ]
\end{aligned}
\tag{1}
$$

https://doi.org/10.5194/wes-2026-218
Preprint. Discussion started: 24 November 2026
© Author(s) 2026. CC BY 4.0 License.



eawe european academy of wind energy
Open Access WIND ENERGY SCIENCE DISCUSSIONS

with A indicating the designated area for the wind farm, defined by the square delimited by $x \in [-3405.9, 3405.9]$ m and $x \in [-3405.9, 3405.9]$ m. The optimization problem is solved using the gradient-free COBYLA optimization solver (Zhang et al., 2023) in OpenMDAO (Gray et al., 2019), setting the tolerance and the maximum number of iterations to 0.1 and 100, respectively.

The solution of the optimization problem is reported in Table 3. Using the optimal values of Δx, Δy, α, and β, the corresponding wind farm layout is reconstructed and visualized in Fig. 7a. The resulting configuration shows that the turbines are not arranged to maximize the utilization of the available area. This spatial distribution reduces wake interactions within the wind farm, thereby minimizing wake losses and maximizing overall power production.

Table 3. Solution of the wind farm layout optimization problem.

Parameter	Symbol	Optimal value	Unit
Primary spacing	$\Delta y'$	7.74	-
Secondary spacing	$\Delta x'$	6.27	-
Orientation angle	α	2.66	deg
Skew angle	β	-2.66	deg
Substation x coordinate	x_{sub}	51.0	m
Substation y coordinate	y_{sub}	25.2	m

3.2 Solar PV

The objective of the solar PV farm design is to define a technically robust and consistent reference design that reflects the operational constraints of a grid-connected hybrid system with wind generation and battery energy storage. The assumptions used for the design are aligned with the system-level parameters of the HPP and form the basis for sizing the PV DC capacity, selecting the module, and defining the inverter topology and electrical architecture used in subsequent analyses.

Depending on the goal of the solar PV design, the choice for DC/AC ratio will vary between 1 and 1.6, as oversizing the PV DC capacity can be beneficial to increase annual energy yield, improve inverter utilization during low-irradiance periods, and reduce the relative impact of grid and inverter clipping. In HPPs with wind generation and battery energy storage, higher DC/AC ratios also allow excess PV production to be absorbed by the battery rather than curtailed, thereby enhancing storage utilization and overall system dispatch flexibility. However, beyond a certain level of DC oversizing, the marginal energy gains decrease due to increasing curtailment and limited storage capacity, meaning the optimal DC/AC ratio must be determined through system-level simulations that balance additional capital expenditure against incremental energy and revenue gains.

We selected a PV module with a nominal power rating of 640 Wp and with the electrical characteristics listed in Table 4. For our case, as mentioned in Section 2.3, the optimal DC/AC ratio is 1; therefore, our PV DC capacity would be 400 MWp, requiring approximately 625,000 installed modules.

https://doi.org/10.5194/wes-2026-218
Preprint. Discussion started: 24 November 2026
© Author(s) 2026. CC BY 4.0 License.

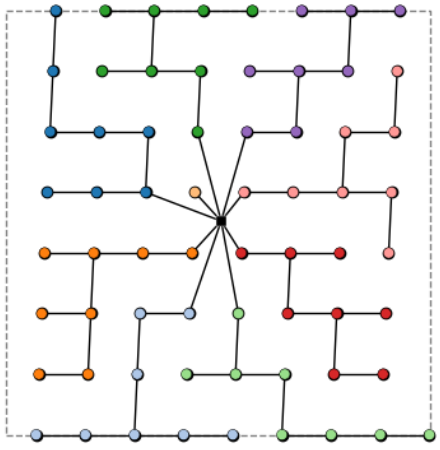

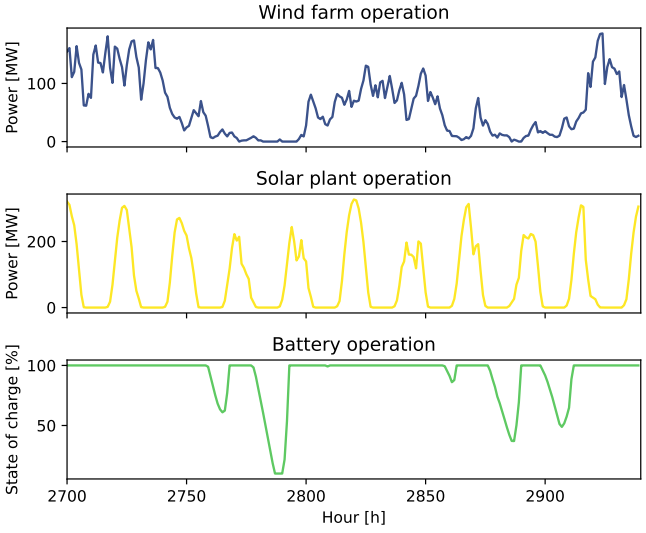

(a) Wind farm layout and cabling connections. The different cable strings are plotted with different colours, and the substation is indicated by the black dot.

(b) 10-day example of the HPP operation obtained from optimized wind farm.

Figure 7. Optimal wind farm design and HPP operation according to H2Integrate.

Table 4. PV module electrical characteristics

Nominal rated power	640 Wp
Open-circuit voltage (Voc)	53.7 V
Voltage at maximum power (Vmp)	44.36 V
Current at maximum power (Imp)	14.43 A
Short-circuit current (Isc)	15.13 A
Temperature coefficient of Voc	-0.20%.^{o}C^{-1}

The plant employs centralized medium-voltage inverters, each with a nominal AC capacity of 6.8 MW. A total of 59 inverters are required to achieve the target AC capacity. Each inverter integrates multiple maximum power point tracking (MPPT) inputs, with the DC field arranged into strings and combiners as follows:

- 25 modules per string, selected to remain within inverter voltage limits under minimum ambient temperature conditions
- String configuration validated against corrected cold-temperature open-circuit voltage values using a minimum ambient temperature of -30 °C
- 425 strings per inverter, distributed across MPPT inputs; those strings are divided into multiple combiner boxes and distributed as reported in Table 5.

https://doi.org/10.5194/wes-2026-218
Preprint. Discussion started: 24 November 2026
© Author(s) 2026. CC BY 4.0 License.



eawe european academy of wind energy
Open Access WIND ENERGY SCIENCE DISCUSSIONS

Table 5. Distribution of strings across MPPT inputs.

MPP	Strings/MPP	Combiner boxes with 10 strings	Combiner boxes with 7 strings	Combiner boxes with 6 strings
MPP1	107	10	1	0
MPP2	106	10	0	1
MPP3	106	10	0	1
MPP4	106	10	0	1
Total	425	40	1	3

Table 6. Characteristics of the battery unit.

Energy capacity	5.015 MWh
Nominal power (0.5C)	2.5 MW
DC round-trip efficiency at nominal rate	93.7%
DC round-trip efficiency at 0.25C	95.2%

3.3 Storage system

Electrochemical storage systems based on batteries are the state-of-the-art energy storage approach for HPPs and short-term grid applications. Of the battery types available, lithium-ion technologies are widely used because of their high efficiency and ability to withstand cycling (charging and discharging).

Another advantage of lithium-ion batteries is their large charge/discharge ratio compared to other technologies. With rates of up to 4 C (Lai et al., 2024) (meaning that the battery can theoretically be fully discharged in about 1/4 of an hour), lithium-ion batteries provide great advantages for power applications. For the typical use cases of a HPP in an energy management mode, discharge rates of 0.25C to 0.5C are typical (which means the storage system will be able to charge/discharge in 2 to 4 hours) and well within the specifications of this battery system. As explained by Lai et al. (2024), the efficiency of the battery system with lithium-ion technology remains stable, although at larger discharge rates the efficiency decreases because of the increased heat generation from the batteries' resistive components.

The selected storage system is based on lithium-ion battery units using a lithium-iron-phosphate chemistry with characteristics provided in Table 6. These data are based on the containerized solution of TESVOLT AG (2025) since it is representative of the state of the art and its technical specifications are available. The proposed storage solution provides a power conditioning unit with a maximum efficiency of 98.6%. The cycling lifetime of the battery is 11,000 full-load cycles, assuming a final state-of-health of 60%. Based on the DC round-trip efficiency and the efficiency of the power conversion unit, nominal AC round-trip efficiency of 91% is assumed.

Containerized storage systems are common because they are easy to deploy and have low installation costs. They are modular, similar to PV systems, and provide increased reliability if the grid is designed for it (e.g. ring configurations). To match the

https://doi.org/10.5194/wes-2026-218
Preprint. Discussion started: 24 November 2026
© Author(s) 2026. CC BY 4.0 License.



eawe european academy of wind energy
Open Access WIND ENERGY SCIENCE DISCUSSIONS

energy and power capacity of the system-level design (see Table A1) in this reference design, the total storage system is made of 60 battery units.

3.4 Shared infrastructure

Power utilities need certain infrastructure elements irrespective of the generation technology. An HPP, by definition, combines multiple co-located technologies. Such joined technologies can share the adjacent infrastructure necessary for reliable and safe grid connection.

From an electrical perspective, shared infrastructure may include medium-voltage cable networks, transformer substations, earthing systems, switchgear, auxiliary transformers, surge arresters, busbars, SCADA and fiber-optic communication systems, capacitor banks, auxiliary generators, and static synchronous compensators. From a civil engineering perspective, co-location can reduce costs related to access and transportation roads, warehouses, operation and control buildings, cable trenches, excavation works, fencing, and fire protection systems.

In this reference design, the technologies are intentionally kept mostly electrically and civilly decoupled within the power plant. This means that different technologies have separate electrical designs and are being joined at the transformer substation point. As a result, potential cost benefits of shared infrastructure are not explicitly addressed (such as those mentioned previously: cable networks, earthing system, roads, cable trenches, etc.). The proposed design instead provides a neutral, more conventional, baseline. This allows future studies to quantitatively assess the benefits of shared infrastructure in reference to the industry standard practice.

In addition to physical infrastructure, HPPs require coordinated control through a common plant controller. The design of the plant can influence plant control and performance, and vice versa. For instance, if the choice of medium-voltage cable cross sections is based on the nameplate capacities of generating technologies, large distances between the grid connection point and individual technologies would increase the voltage drops at the controller reference point. This prompts the designer to choose a larger cross section, even though from thermal characteristics of such cable there is no need to do so. This clearly shows how the design can impact the operation, and how the proper operation considerations impact the proper choice of the components. The following section explains the operational criteria and the resulting electrical design and resulting parameters.

3.4.1 The electrical network in the HPP

The grid design is focused on basic design parameters such as cable type and cross section with the following design criteria:

- Maximum voltage deviation between the common connection point and the farthest generation unit of no more than 5%
- Maximum power losses on cabling of less than 5%
- Fixed transformer impedance of 0.01 + j0.1 p.u.

https://doi.org/10.5194/wes-2026-218
Preprint. Discussion started: 24 November 2026
© Author(s) 2026. CC BY 4.0 License.

In order to keep the cable design to a manageable cross section, the nominal voltage has been selected to be 33 kV. Because of the long distances between the different plant sections (PV, wind and battery), it is advised to step up the plant voltage. For the sake of staying at the medium voltage level (below 35 kV), the design is completely done for 33 kV.

As explained in the previous section, the plant has been designed to be spatially separate as shown in Fig. 8. It is, however, electrically connected to the same transforming station to fulfil the definition of an HPP. An advantage of having separate subgrids for each generating cluster lies in the plant controller design. As reported in Notholt et al. (2025), there are several concepts for a hybrid plant control. One of the easiest to implement is a cascaded control concept, which in turn usually requires the secondary controllers to measure the actual injected power. This can be easily implemented with the proposed grid configuration. One drawback, however, is the fact that the distance between each cluster's optimal position of the substation and the grid connection is quite large, thus requiring larger cross sections. All three technological clusters (wind, PV, and storage) are directly connected at the substation level to a 6-field switchgear.

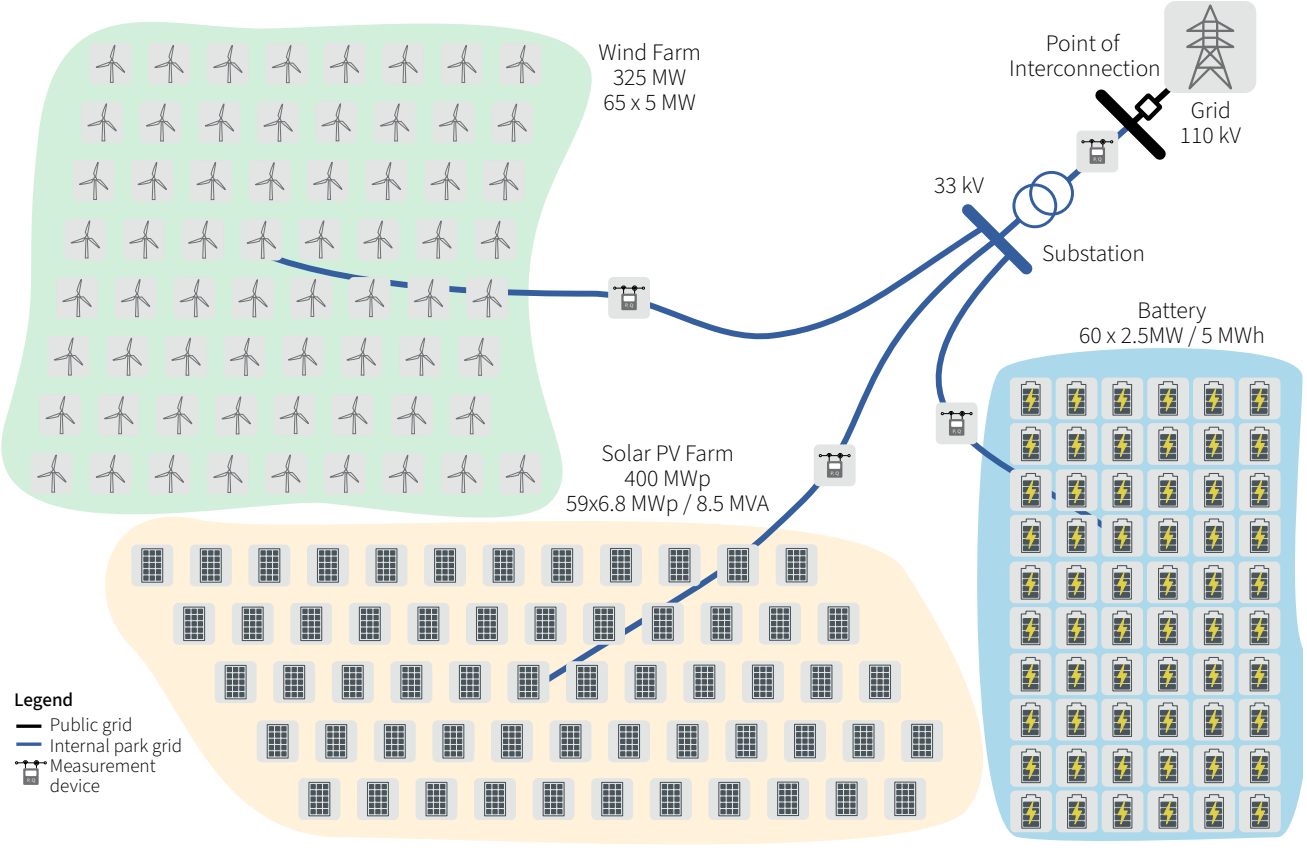

Figure 8. Proposed grid configuration.

https://doi.org/10.5194/wes-2026-218
Preprint. Discussion started: 24 November 2026
© Author(s) 2026. CC BY 4.0 License.



eawe european academy of wind energy
Open Access WIND ENERGY SCIENCE DISCUSSIONS

The standard cabling on wind and PV power plants involves underground cables, typically aluminum with XLPE isolation, 90°C, 36 kV. To reduce effort, only four standard cable cross sections (described in Table 7) have been considered. This reduces not only the effort but also the installation complexity.

Table 7. Selected cables and ratings per ELAND Cables (2026).

Cross section	Ampacity (A)*	R (Ω/km)	L** (Ω/km)	C (μF/km)	Use
150 mm^2	361	0.269	0.124	0.194	String ends (1–3 units***)
240 mm^2	469	0.166	0.115	0.231	Intermediate (4–5 units)
400 mm^2	590	0.106	0.103	0.305	String base (6–7 units)
630 mm^2	730	0.065	0.083[a]	0.407[a]	String to common feeder

* Ampacity for trefoil configuration directly buried into the ground, ** Impedance for trefoil configuration at 50 Hz, *** Wind turbines, PV, battery container, [a] Extrapolated

4 Operation and performance

In this section, we present an example of use for the reference design. For this, we formulate a standard dispatch optimization problem to simulate the operation of the HPP (Section 4.1) and use it to evaluate the economic performance of the power plant (Section 4.2).

4.1 Energy management system

The EMS of an HPP sets the dispatch schedule to be followed to maximize electricity delivery and revenues on the electricity markets and reduce curtailment.

Here, the EMS is modelled as a dispatch optimization problem. The objective is to maximize electricity revenue. The decision variables are the time series of curtailed power ($\boldsymbol{P}^{\mathrm{C}}$), storage system power in charge ($\boldsymbol{P}^{\mathrm{S-}}$) and discharge ($\boldsymbol{P}^{\mathrm{S+}}$), and state of charge ($\boldsymbol{E}$). In addition to the storage model, constraints are set on the power and energy capacity of the storage system and the maximum grid capacity. The initial and final state of charge are set to be equal to avoid the battery being emptied at the end of the time period. In mathematical terms, the problem is

https://doi.org/10.5194/wes-2026-218
Preprint. Discussion started: 24 November 2026
© Author(s) 2026. CC BY 4.0 License.



eawe european academy of wind energy
Open Access WIND ENERGY SCIENCE DISCUSSIONS

$$
\begin{aligned}
\max_{\boldsymbol{P}^{\text{S-}},\boldsymbol{P}^{\text{S+}},\boldsymbol{E},\boldsymbol{P}^{\text{C}}} \quad & \sum_{i=1}^{n} \lambda_i (P_i^{\text{S+}} - P_i^{\text{S-}} - P_i^{\text{C}})\Delta t + \epsilon (P_i^{\text{S+}} + P_i^{\text{S-}})\Delta t \\
\text{subject to} \quad & 0 \le P_i^{\text{WF}} + P_i^{\text{PV}} + P_i^{\text{S+}} - P_i^{\text{S-}} - P_i^{\text{C}} \le \bar{P}^{\text{HPP}} && i = 1,...,n \\
& P_i^{\text{S+}} - P_i^{\text{S-}} \le \max(\bar{P}^{\text{HPP}} - P_i^{\text{WF}} - P_i^{\text{PV}}, 0) && i = 1,...,n \\
& 0 \le P_i^{\text{S+}} \le \bar{P}^{\text{S}} && i = 1,...,n, \\
& 0 \le P_i^{\text{S-}} \le \bar{P}^{\text{S}} && i = 1,...,n, \\
& (1-d)\bar{E} \le E_i \le \bar{E} && i = 1,...,n+1, \\
& E_{i+1} - E_i = \eta \Delta t P_i^{\text{S-}} - \frac{\Delta t}{\eta} P_i^{\text{S+}} && i = 1,...,n, \\
& E_1 \le E_{n+1},
\end{aligned}
\tag{2}
$$

where Δt is the time step duration, λ_i is the price of selling one unit of energy at time step i, $\bar{E}$ is the energy capacity of the battery, $\bar{P}^s$ is the power capacity, d is the depth of charge, and $\boldsymbol{P}^{\text{PV}}$ and $\boldsymbol{P}^{\text{WF}}$ are the power production from the solar PV and wind farm, respectively. The parameter $\epsilon = 10^{-3}$ serves as a regularization term to avoid simultaneous charging and discharging.

The dispatch optimization problem is solved for one year of operation with $n = 8760$, with an hourly time increment $\Delta t = 1$ and a depth of charge of 90%. The wind farm and solar PV farm power are generated following the models described in the previous section with weather input data from 2022. The wind farm is modelled in FLORIS via H2Integrate, and the solar PV farm is modelled in pvlib with the PVWatts and CEC models. Since 2022 was characterized by unusually high prices in the day-ahead electricity market (average 220 EUR.MWh^{-1}), using historical prices would lead to nonrepresentative results. Instead, an artificial price signal is generated from the time series of wind speed, following the methodology of Mehta et al. (2024). The resulting signal has a mean price of 33 EUR.MWh^{-1}, a coefficient of variation of 0.45, and a correlation of -0.37 with the wind speed, representing the characteristics of the period 2016 to 2020. The problem is implemented in the open-source code SHIPP v1.2.2 (Iori, 2025) and solved using the optimization algorithm HIGHS (Huangfu et al., 2026) and the Python package `scipy.linprog`.

Figure 9 illustrates two periods of 3 days of operation. The wind farm power production is high in January and relatively lower in June, whereas the opposite is observed for the solar PV production. In both case, the total power production occasionally exceeds the grid capacity. This is handled with the EMS by curtailing the power or charging the storage system. In addition to curtailment periods, the storage system charges and discharges power to take advantage of price differentials.

4.2 Performance metrics

Using the operational schedule calculated by the EMS, the operational performance metrics of the power are calculated and reported in Table 8. The wind and solar PV farms have a capacity factor of 40.3% and 12.0%, respectively. Curtailment represents a small share of the total produced energy at 5%. However, the grid utilization factor is around 55%, demonstrating

https://doi.org/10.5194/wes-2026-218
Preprint. Discussion started: 24 November 2026
© Author(s) 2026. CC BY 4.0 License.

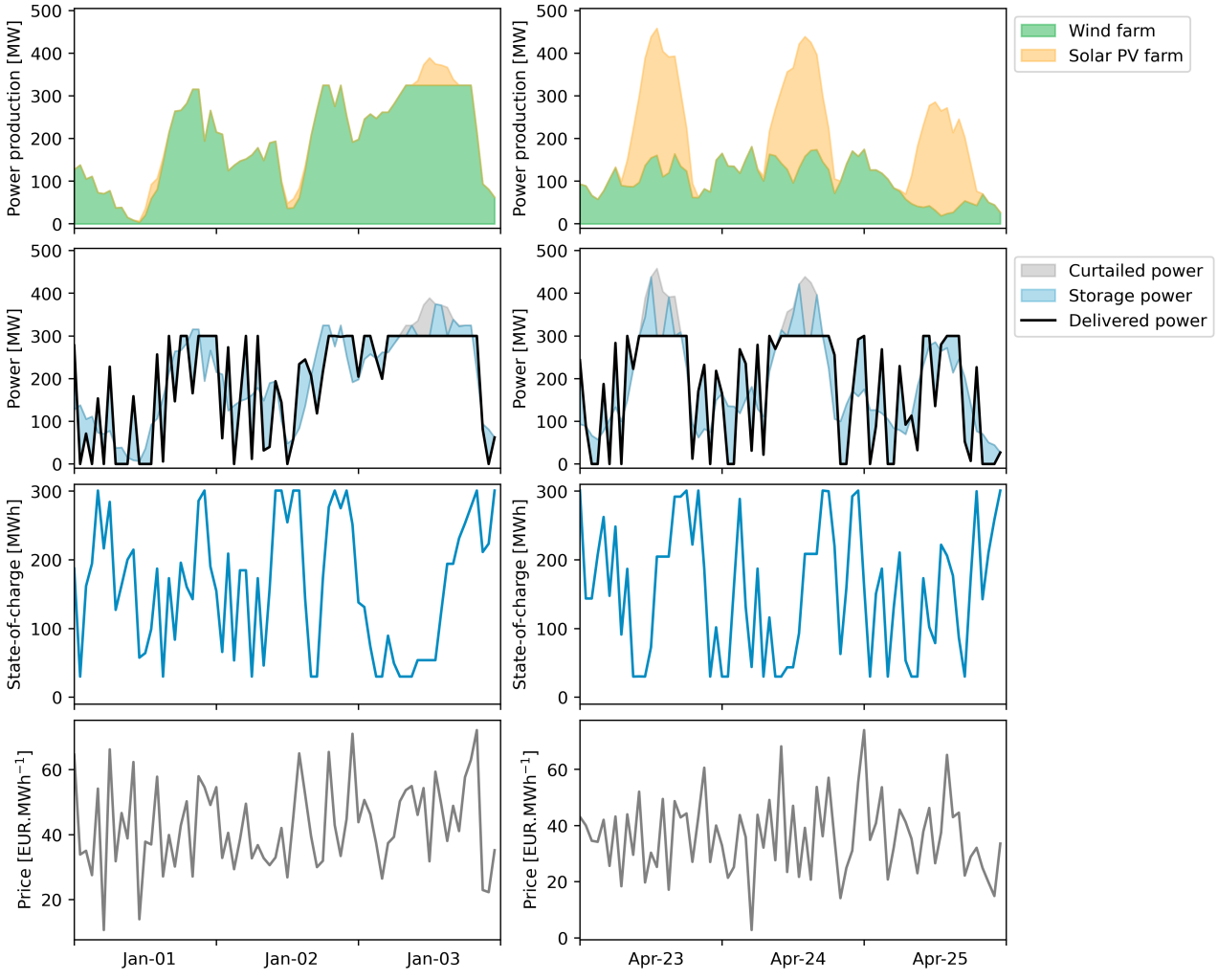

Figure 9. Example of EMS results for 3 days in January (left) and June (right): (from top to bottom) power produced from the solar PV and wind farm, power delivered to the grid, state of charge of the storage system, and electricity price.

https://doi.org/10.5194/wes-2026-218
Preprint. Discussion started: 24 November 2026
© Author(s) 2026. CC BY 4.0 License.



eawe european academy of wind energy
Open Access WIND ENERGY SCIENCE DISCUSSIONS

Table 8. Operational performance metrics for the year 2022.

Annual energy production (AEP) wind [GWh]	1148.6
AEP solar PV [GWh]	419.9
AEP HPP [GWh]	1461.8
Total curtailment [GWh]	82.4
Battery losses [GWh]	24.3
Grid utilization factor [%]	55.5

Table 9. Cost assumptions for the year 2030 (Danish Energy Agency, 2025a, b).

	Wind farm	Solar PV farm	Battery	Shared costs
CAPEX [EUR.kW^{-1}]	946	290	84	290
CAPEX [EUR.kWh^{-1}]	-	-	195	-
OPEX [EUR.kW^{-1}]	16.6	9.5	8.0	-

the ability of the HPP to make optimal use of the limited available capacity. Finally, revenues generated from the storage operation represent approximately 11% of the total.

Financial performance metrics for the power plant are calculated assuming a lifetime of 25 years, with a real weighted average cost of capital of 3.9%. The battery is replaced twice during the project duration due to degradation, but the impact of degradation on performance is not modelled. Replacement of the other components of the power plant is not considered. Using the cost assumptions listed in Table 9, the total CAPEX is 673 million EUR, leading to a LCOE of 36.3 EUR.MWh^{-1}. Further financial metrics are reported in Table 10. Details of the cost breakdown and financial metric calculation are reported in Appendix B. Since the revenues of the power plant are sensitive to the assumption on the mean electricity price, the calculation is done for three different values: 33 EUR.MWh^{-1} representative of the period 2016 to 2020, 72 EUR.MWh^{-1} representative of the period 2016 to 2025, and a middle point of 45 EUR.MWh^{-1}. The power plant demonstrates good performance in all scenarios.

Table 10. Financial metrics of the reference design for different assumptions of the mean electricity price.

Mean electricity price [EUR.MWh^{-1}]	33	45	72
Annual revenues [M.EUR]	55.5	75.7	121.1
Storage revenues [M.EUR]	5.3	7.2	11.5
NPV/CAPEX [-]	0.058	0.532	1.598
NPV [M.EUR]	39	358	1075
IRR [%]	4.5	9.1	18.0

https://doi.org/10.5194/wes-2026-218
Preprint. Discussion started: 24 November 2026
© Author(s) 2026. CC BY 4.0 License.



eawe european academy of wind energy
Open Access WIND ENERGY SCIENCE DISCUSSIONS

5 Dataset format and organization

The reference design is described using several YAML files using a format adapted from the WindIO scheme (Bortolotti et al., 2026). This format allows data to be stored in a "human-readable" format and is widely used for the description of reference wind turbines and wind farms. The dataset is divided into several components:

- Wind farm description, with the site boundaries, the coordinates of the wind turbines and substation, the layout of the electrical collection network, and the turbine characteristics (power coefficient and thrust curve, hub height, rotor diameter)
- Solar PV farm description, with the characteristics of the PV modules, number of modules per string and strings per inverter, inverter characteristics, and the orientation of the modules
- Storage system description, with the round-trip efficiency, cycling lifetime, efficiency of the power conditioning unit, and power and energy capacities.

6 Discussion

The reference HPP presented in this work represents a combination of technologies chosen for specific design problem boundaries. In particular, the choice of 300 MW grid connection capacity drives the rest of the design. Therefore, it may be impractical to use the reference design for studies with a different grid capacity. However, the modularity of the solar PV farm and the storage system allows a straightforward scaling of power capacity. For the wind farm design, the regular grid layout enables scaling power capacity by adding or removing individual turbines or entire rows and columns. For example, removing the 29 turbines closest to the boundaries of the farm reduces the power rating to 180 MW without affecting the relative alignment of the turbines to the wind direction.

In order to use the reference design on a different site, two adjustments are recommended. First, the wind farm layout should be rotated so that the turbine main direction of alignment is orthogonal to the main wind direction (or, preferably, the wind farm grid layout should be reoptimized for the new site). Second, the orientation of the solar PV modules should be recalculated to optimize power production.

This design is generated and evaluated using several design and analysis tools. HyDesign is used for the generation of the system-level parameters of the plant. H2Integrate and Ard are used to generate the wind farm layout. Finally, SHIPP is used for the EMS simulation and evaluation of the performance metrics. These two tools are very similar in their capacity and the fidelity of the models implemented, raising the question of the rational behind their use. This can be explained with the context of IEA Wind TCP Task 50. The tasks to generate the reference design were divided among participants and conducted using the preferred toolchain at each participant's institution. Using different models to refine the design initially found using HyDesign may affect the optimality of the power plant (either positively or negatively). However, the goal of this dataset is to present an example HPP design, not necessarily an optimal one.

https://doi.org/10.5194/wes-2026-218
Preprint. Discussion started: 24 November 2026
© Author(s) 2026. CC BY 4.0 License.



eawe european academy of wind energy
Open Access WIND ENERGY SCIENCE DISCUSSIONS

One important aspect of the design process is the choice of reference year for the time series of wind and solar resource. The year 2022 was chosen because of the availability of 15-minute forecast data from that year onwards. Furthermore, choosing this reference year enable studies simulating the design and operation phase separately while having historical wind and solar resource data available. This would not be possible if the design was generated with 2025 data.

We note that using a time series of one year of data is uncommon for both wind farm and solar PV farm design. Wind farm design studies are generally conducted based on sectoral Weibull distributions in order to represent long-term trends in the wind resource. For similar reasons, solar PV studies make use of a typical meteorological year. These two approaches are unpractical for HPP design since the temporal correlation between the two resources is important for the performance of the power plant. Furthermore, evaluation of the storage system performance requires an analysis in the time domain in order to capture the coupling between state of charge and charge/discharge cycles.

7 Conclusions

We present and make available the specifications of a reference design for HPPs. The power plant is made of a 325 MW wind farm, a 400 MW solar PV farm and a 150 MW and 300 MWh battery, co-located behind a 300 MW grid connection. The detailed design of each component of the power plant is provided. The wind farm is characterized by its layout, collection system, and turbine characteristics. We provide the properties of the solar PV module and electrical infrastructure of the solar PV farm. We present a battery unit with its chemistry, nominal capacity, and DC round-trip efficiencies at different operation points. Finally, we show how the components are connected with a description of the shared electrical infrastructure.

This dataset provides a high level of detail in each component design in order to conduct advanced simulations of the HPP, thereby providing a solid basis for further research on, and development of, HPPs.

Code and data availability. The dataset is available open-source in the GitHub repository: github.com/IEAWindTask50/hpp-reference-designs. Example scripts are provided to showcase the use of the dataset.

Appendix A: Additional wind farm design details

Because the wind farm was designed with the full system in mind but modelled in H2Integrate (Brunik et al., 2025), there are some unique inputs and outputs compared to the rest of the HPP analysis performed in this paper. Extra inputs and outputs from H2Integrate are provided in the appendix to avoid confusion in the main body of the paper.

Additional input details are provided in Table A1. Some additional description may be helpful for some of the parameters given. The peak shaving fraction reduces the thrust from the peak thrust on the nominal thrust curve, only affecting wind speeds near the peak in the thrust. The branched collection topology allows the cable array to branch at nodes other than the substation. The max turbines per string limits how many turbines can be placed along a single string (including branches) in

https://doi.org/10.5194/wes-2026-218
Preprint. Discussion started: 24 November 2026
© Author(s) 2026. CC BY 4.0 License.



eawe european academy of wind energy
Open Access WIND ENERGY SCIENCE DISCUSSIONS

the cable array. The bifaciality is a multiplier for the solar rear irradiance for bifacial solar panels (panels that collect on both sides).

Table A1. Summary of H2Integrate inputs for the wind farm design.

Technology	Parameter	Value	Units
Wind	Peak shaving fraction	0.2	
	Collection topology	branched	
	Max turbines per string	8	
	Turbine rating	5	MW
	Cost year	2024	year
	Turbine capital cost	1300	USD.kW^{-1}
	OPEX	44	USD.kW^{-1}
	Commissioning cost	44	USD.kW^{-1}
	Decommissioning cost	58	USD.kW^{-1}
Solar	PV capacity	400	MW
	Tilt	25	deg
	GCR	0.3	
	Azimuth	180	deg
	Bifaciality	0.65	
	Inverter efficiency	96	percent
	Losses	14.6	percent
	Cost year	2020	year
	CAPEX	269.1	USD.kW^{-1}
	OPEX	4.5	$(\text{USD.kW}^{-1}).\text{year}^{-1}$
Battery	Max charge rate	150	MW
	Max discharge rate	150	MW
	Max capacity	300	MWh
	Max/min/init charge	1/0.1/0.25	
	Charge/discharge efficiency	0.985	
	Cost year	2020	year
	Energy CAPEX	72.54	USD.kWh^{-1}
	Power CAPEX	115	USD.kW^{-1}
	OPEX fraction	0	
Grid	Constant demand	300	MW

405 An example of the operation of the optimized wind farm design and the other components of the HPP are depicted in Fig. 7b. The figure refers to a 10-day time series of power production of both the wind and PV plants, together with the state of charge

https://doi.org/10.5194/wes-2026-218
Preprint. Discussion started: 24 November 2026
© Author(s) 2026. CC BY 4.0 License.



eawe european academy of wind energy
Open Access WIND ENERGY SCIENCE DISCUSSIONS

of the battery. These results show how the battery is discharged when the the wind farm power production is limited during periods of low wind resources.

Lastly, Table A2 summarizes the performance metric values of the HPP with the optimized wind farm layout, which are calculated with the models adopted during the optimization.

Table A2. H2Integrate operational and financial performance metrics.

Metric	Value	Unit
AEP wind farm	1148.6	GWh
Capacity factor wind farm	0.403	-
AEP PV plant	446.0	GWh
Capacity factor PV plant	0.127	-
LCOE HPP	0.303	USD.kWh^{-1}
Weighted average cost of capital HPP	6.25	%
Capital recovery factor HPP	7.65	%
IRR HPP	9	%

Appendix B: Description of the cost data and financial metrics

The cost assumptions used in this study are based on data from Danish Energy Agency (2025a, b). This dataset reports details of the cost breakdown of different components when built individually but not when part of a co-located facility. To model the shared infrastructure costs of HPPs, the costs of the wind farm and solar PV farm have been divided into a part proportional to the rated capacity of the individual component and a part proportional to the HPP grid capacity, representing shared costs. We assume that these shared costs are the sum of costs from the individual component cost estimation. This leads to a conservative analysis, as we do not take into account potential cost reductions from reusing the same infrastructure. Table B1 reports how the different costs are obtained from the original data.

The CAPEX of the HPP is made of four components: the wind farm (WF), the solar PV farm (PV), the storage system (S) and shared costs (SC). For each component, the CAPEX $C^{\square}$ is calculated using the cost per power capacity (or rated power) $\lambda_p^{\square}$ multiplied by the rated power of the component $\bar{P}^{\square}$. For the storage system, the CAPEX also depends on the energy capacity $\bar{E}$ through the cost per energy capacity λ_E^S.

$$C^{\text{WF}} = \lambda_P^{\text{WF}} \bar{P}^{\text{WF}} \tag{B1}$$

$$C^{\text{PV}} = \lambda_P^{\text{PV}} \bar{P}^{\text{PV}} \tag{B2}$$

$$C^{\text{SC}} = \lambda_P^{\text{SC}} \bar{P}^{\text{HPP}} \tag{B3}$$

$$C^{S} = \lambda_E^S \bar{E} + \lambda_P^S \bar{P}^{S} \tag{B4}$$

https://doi.org/10.5194/wes-2026-218
Preprint. Discussion started: 24 November 2026
© Author(s) 2026. CC BY 4.0 License.



eawe european academy of wind energy
Open Access WIND ENERGY SCIENCE DISCUSSIONS

Table B1. Breakdown of the cost assumptions for the wind farm, solar PV farm, battery and shared costs listed in Table 9. All costs are based on 2030 data from Danish Energy Agency (2025a, b)

Onshore turbines - Nominal investment (equipment) [EUR.kW^{-1}]	828
Onshore turbines - Nominal investment (installation/development) [EUR.kW^{-1}]	86
Onshore turbines - Nominal investment (decommissioning of existing turbines) [EUR.kW^{-1}]	32
Total Wind CAPEX [EUR.kW^{-1}] (λ_P^{WF})	846
Utility-scale PV - Nominal investment (inverter) [EUR.kW^{-1}]	20
Utility-scale PV - Nominal investment (pv modules) [EUR.kW^{-1}]	140
Utility-scale PV - Nominal investment (installation) [EUR.kW^{-1}]	100
Utility-scale PV - Nominal investment (soft costs) [EUR.kW^{-1}]	30
Total Solar PV CAPEX [EUR.kW^{-1}] (λ_P^{PV})	290
Onshore turbines - Nominal investment (grid connection) [EUR.kW^{-1}]	20
Onshore turbines - Nominal investment (purchase of neighbour settlements) [EUR.kW^{-1}]	70
Onshore turbines - Nominal investment (land purchase/rent) [EUR.kW^{-1}]	110
Utility-scale PV - Nominal investment (grid connection) [EUR.kW^{-1}]	50
Utility-scale PV - Nominal investment (other, i.e. residual balance of plant) [EUR.kW^{-1}]	40
Total Shared cost CAPEX [EUR.kW^{-1}] (λ_P^{SC})	290
Lithium-ion Battery - Energy component costs [EUR.kWh^{-1}]	65
Lithium-ion Battery - Other project costs [EUR.kWh^{-1}]	130
Total battery CAPEX [EUR.kWh^{-1}] (λ_E^{S})	195

The total CAPEX is calculated taking into account the two battery replacement at years $m_S = 8$ and $2m_S = 16$, with a discount of the corresponding costs at rate r.

$$\mathrm{CAPEX}^{\mathrm{HPP}} = C^{\mathrm{WF}} + C^{\mathrm{PV}} + C^{\mathrm{SC}} + C^{\mathrm{S}}(1 + \frac{1}{(1+r)^{m_{\mathrm{S}}}} + \frac{1}{(1+r)^{2m_{\mathrm{S}}}}). \tag{B5}$$

The total OPEX is made of the OPEX costs for the wind farm, solar PV farm and storage system, all proportional to their rated power through the OPEX per power capacity $\lambda_O^{\square}$:

$$\mathrm{OPEX}^{\mathrm{HPP}} = \lambda_O^{\mathrm{WF}} \bar{P}^{\mathrm{WF}} + \lambda_O^{\mathrm{PV}} \bar{P}^{\mathrm{PV}} + \lambda_O^{\mathrm{S}} \bar{P}^{\mathrm{S}}. \tag{B6}$$

The annual revenues of the power plant R are calculated as the dot product of the delivered power with the vector of electricity price $\boldsymbol{\lambda}$,

$$R = \boldsymbol{\lambda}^T(\boldsymbol{P}^{\mathrm{WF}} + \boldsymbol{P}^{\mathrm{PV}} + \boldsymbol{P}^{\mathrm{S+}} - \boldsymbol{P}^{\mathrm{S-}} - \boldsymbol{P}^{\mathrm{c}})\Delta t. \tag{B7}$$

The NPV is calculated as the sum of discounted cash flow during the lifetime of the power plant. We assume that the HPP is installed during year 0 and operates between year 1 and $m = 25$. During each year of operation, we only consider the revenues

https://doi.org/10.5194/wes-2026-218
Preprint. Discussion started: 24 November 2026
© Author(s) 2026. CC BY 4.0 License.



eawe european academy of wind energy
Open Access WIND ENERGY SCIENCE DISCUSSIONS

from electricity sales and OPEX costs in the cash flow. Furthermore, the annual revenue is assumed to be the same during the lifetime of the project, neglecting degradation effects and year-to-year variations. Mathematically, the NPV is calculated as

$$\text{NPV} = -\text{CAPEX}^{\text{HPP}} + \sum_{k=1}^{m} \frac{R - \text{OPEX}^{\text{HPP}}}{(1+r)^k}. \tag{B8}$$

The LCOE is calculated as the ratio between the levelized AEP and the levelized costs, using the following formula

$$\text{LCOE} = \frac{\sum_{k=1}^{m} \frac{\text{AEP}^{\text{HPP}}}{(1+r)^k}}{\text{CAPEX}^{\text{HPP}} + \sum_{k=1}^{m} \frac{\text{OPEX}^{\text{HPP}}}{(1+r)^k}}, \tag{B9}$$

where the AEP is calculated as the sum of delivered power, and thus includes curtailment and storage system losses,

$$\text{AEP}^{\text{HPP}} = \sum_{i=1}^{n} (P_i^{\text{WF}} + P_i^{\text{PV}} + P_i^{\text{S+}} - P_i^{\text{S-}} - P_i^{\text{C}}) \Delta t. \tag{B10}$$

Author contributions. All co-authors contributed to conceptualization of the work by participating in discussions on the goal of the reference design and refining the problem boundaries. MG provided the preliminary design of the HPP. MB and JT provided the wind farm and cable layout. RBG provided the solar PV module and farm specifications. AN provided the specifications of the battery system and electrical components. AN and KO provided the discussion on the shared infrastructure. JI ran the numerical experiments for the operation and performance. MG, MB, JT, RGB, AN, KO and JI wrote the section corresponding to the part of the design they worked on. DP critically reviewed and edited the draft. KO and JI coordinated the writing effort. JI supervised the work as work package lead. CB and KD managed and coordinated IEA Task 50 as operating agents. All co-authors reviewed the paper.

Competing interests. The authors declare no competing interests.

Acknowledgements. This work was conducted as part of work package 2 of the IEA Wind TCP Task 50 on hybrid power plant reference design. The authors would like to thank all participants of the work package for their input during meetings and discussions, that helped define and refine the reference design.

Furthermore, the authors would like to thank Xin Yuan (TU Delft) for input on the site characteristics section.

This work was authored in part by the National Laboratory of the Rockies for the U.S. Department of Energy (DOE), operated under Contract No. DE-AC36-08GO28308. Funding provided by U.S. Department of Energy Office of Critical Minerals and Energy Innovation Integrated Energy Systems Office. The views expressed in the article do not necessarily represent the views of the DOE or the U.S. Government. The U.S. Government retains and the publisher, by accepting the article for publication, acknowledges that the U.S. Government

https://doi.org/10.5194/wes-2026-218
Preprint. Discussion started: 24 November 2026
© Author(s) 2026. CC BY 4.0 License.



eawe european academy of wind energy
Open Access WIND ENERGY SCIENCE DISCUSSIONS

retains a nonexclusive, paid-up, irrevocable, worldwide license to publish or reproduce the published form of this work, or allow others to do so, for U.S. Government purposes.

https://doi.org/10.5194/wes-2026-218
Preprint. Discussion started: 24 November 2026
© Author(s) 2026. CC BY 4.0 License.



eawe european academy of wind energy
Open Access WIND ENERGY SCIENCE DISCUSSIONS

References

Anderson, K. S., Hansen, C. W., Holmgren, W. F., Jensen, A. R., Mikofski, M. A., and Driesse, A.: pvlib python: 2023 project update, Journal of Open Source Software, 8, 5994, https://doi.org/10.21105/joss.05994, 2023.

Bortolotti, P., Mudafort, R. M., Quick, J., Zahle, F., kenloen, Bay, C., Barter, G., dzalkind, Lejeune, M., rsmouradi, amirarasteh1990, Mathieu, A., Schulte, J., madsmpedersen, koendev, and Liao, Y.: IEAWindSystems/windIO: Cut in and cut out, TI, and multi-point coordinates, https://doi.org/10.5281/zenodo.18774325, 2026.

Brunik, K., Grant, E., Thomas, J., Starke, G. M., Martin, J., Ramos, D., Koleva, M., Reznicek, E., Hammond, R., Stanislawski, B., Kiefer, C., Irmas, C., Vijayshankar, S., Riccobono, N., Frontin, C., Clark, C., Barker, A., Gupta, A., Kee, B. J., King, J., Jasa, J., and Bay, C.: H2Integrate: Holistic Hybrids Optimization and Design Tool, https://doi.org/10.5281/zenodo.17903150, 2025.

Danish Energy Agency: Energy storage: technology descriptions and projections for long-tem energy system planning, Danish Energy Agency, 2025a.

Danish Energy Agency: Generation of electricity and district heating: technology descriptions and projections for long-tem energy system planning, Danish Energy Agency, 2025b.

Das, K., Hansen, A. D., Leon, J. P. M., Zhu, R., Gupta, M., Pérez-Rúa, J.-A., Long, Q., Pombo, D. V., Barlas, A., Gocmen, T., Sogachev, A., Koivisto, M., Cutululis, N. A., and Sørensen, P. E.: Research Challenges and Opportunities of Utility-Scale Hybrid Power Plants, Wiley Interdisciplinary Reviews: Energy and Environment, 14, https://doi.org/10.1002/wene.70001, 2025.

Dykes, K., King, J., Diorio, N., King, R., Gevorgian, V., Corbus, D., Blair, N., Anderson, K., Stark, G., Turchi, C., and Moriarty, P.: Opportunities for Research and Development of Hybrid Power Plants, Tech. rep., National Renewable Energy Laboratory, https://www.nlr.gov/docs/fy20osti/75026.pdf., 2020.

ELAND Cables: NA2XS(FL)2Y AD8 Cable 18/30 (36)kV, https://www.elandcables.com/electrical-cable-and-accessories/cables-by-standard/german-mv-cables, 2026.

Frontin, C., Bortolotti, P., Mudafort, R., and Thomas, J.: Ard [SWR-25-18], https://doi.org/10.11578/dc.20250108.1, 2024.

Gray, J. S., Hwang, J. T., Martins, J. R. R. A., Moore, K. T., and Naylor, B. A.: OpenMDAO: An open-source framework for multidisciplinary design, analysis, and optimization, Structural and Multidisciplinary Optimization, 59, 1075–1104, https://doi.org/10.1007/s00158-019-02211-z, 2019.

Hall, M., Lozon, E., Devoy McAuliffe, F., Baudino Bessone, M., Bayati, I., Bowie, M., Bozonnet, P., Castagné, M., Feng, J., Housner, S., Janocha, M. J., Jiang, Z., Kim, Y. Y., Ko, D., Kölle, K., Lee, C. F., Lekkala, M. R., Liang, G., Mahfouz, M. Y., Mohan, M., O'Connell, D., Ong, M. C., Prieur, J., Rajasree, V. R. N., Schnepf, A., Snedker, T., Thurston-Keller, J., and Wright, C.: IEA Wind TCP Task 49 Reference Floating Wind Array Design Basis, Technical Report NREL/TP-5000-89709, National Renewable Energy Laboratory (NREL), https://docs.nlr.gov/docs/fy24osti/89709.pdf, prepared for IEA Wind TCP Task 49 on Integrated Design of Floating Wind Arrays, 2024.

Hersbach, H., Bell, B., Berrisford, P., Biavati, G., Horányi, A., Muñoz Sabater, J., Nicolas, J., Peubey, C., Radu, R., Rozum, I., Schepers, D., Simmons, A., Soci, C., Dee, D., and Thépaut, J.-N.: ERA5 hourly data on single levels from 1940 to present, https://doi.org/10.24381/cds.adbb2d47, 2023.

Huangfu, Q., Galabova, I., Feldmeier, M., and Hall, J. A. J.: HiGHS - high performance software for linear optimization, https://https://highs.dev/, 2026.

IBM: IBM ILOG CPLEX Optimization Studio Community Edition 22.1 (Community), https://www.ibm.com/products/ilog-cplex-optimization-studio, 2024.

https://doi.org/10.5194/wes-2026-218
Preprint. Discussion started: 24 November 2026
© Author(s) 2026. CC BY 4.0 License.

IEA Wind Technology Collaboration Programme: Task 50 – Work Package 1, https://iea-wind.org/task50/t50-wp1/, accessed: 9 March 2026, n.d.

International Energy Agency: Total Installed Power Capacity by Fuel and Technology 2019–2025, Main Case, https://www.iea.org/data-and-statistics/charts/total-installed-power-capacity-by-fuel-and-technology-2019-2025-main-case, license: CC BY 4.0. Accessed: 9 March 2026, 2020.

Iori, J.: SHIPP - A design optimization software for hybrid power plants, https://doi.org/10.4121/2EE36148-369F-4E1F-B770-C86752D7DCA4, 2025.

Jonkman, J., Butterfield, S., Musial, W., and Scott, G.: Definition of a 5-MW Reference Wind Turbine for Offshore System Development, Tech. rep., National Renewable Energy Laboratory (NREL), Golden, CO., https://doi.org/10.2172/947422, 2009.

Kainz, S., Quick, J., {Souza de Alencar}, M., Moreno, S., Dykes, K., Bay, C., Zaaijer, M., and Bortolotti, P.: IEA Wind TCP Task 55: The IEA Wind 740-10-MW Reference Offshore Wind Plants, IEA, https://doi.org/10.2172/2333634, 2024.

Kee, J. and Penev, M.: ProFAST (Production Financial Analysis Scenario Tool) [SWR-23-88], https://doi.org/10.11578/dc.20231211.1, 2023.

Lai, Y.-W., Chi, K.-H., Chung, Y.-H., Liao, S.-W., and Shu, C.-M.: Thermal hazard evaluation of 18650 lithium-ion batteries at various discharge rates, Journal of Loss Prevention in the Process Industries, 89, 105 323, https://doi.org/https://doi.org/10.1016/j.jlp.2024.105323, 2024.

Mehta, M. K., Zaaijer, M., and von Terzi, D.: Designing wind turbines for profitability in the day-ahead market, Wind Energy Science, 9, 2283–2300, https://doi.org/10.5194/wes-9-2283-2024, 2024.

Murcia Leon, J. P., Habbou, H., Friis-Møller, M., Gupta, M., Zhu, R., and Das, K.: HyDesign: a tool for sizing optimization of grid-connected hybrid power plants including wind, solar photovoltaic, and lithium-ion batteries, Wind Energy Science, 9, 759–776, 2024.

National Laboratory of the Rockies (NLR): PySAM Version 7.0.0, github.com/NatLabRockies/pysam, 2025.

National Laboratory of the Rockies (NLR): FLORIS: Flow Redirection and Induction in Steady State, https://doi.org/10.5281/zenodo.2672982, 2026a.

National Laboratory of the Rockies (NLR): WISDEM: Wind-Plant Integrated System Design & Engineering Model, https://github.com/NLRWindSystems/WISDEM, 2026b.

Notholt, A., Balakhontsev, O., Kernstock, L., and Elheni, M. B.: Next Generation Renewable - Diesel-Hybridkraftwerke für die globale Energiewende in netzfernen Regionen; Optimierung der PV-Kraftwerks-, Windpark- und Netztechnik für einen stabilen Netzbetrieb und eine nachhaltige Stromversorgung mit hohen solaren Deckungsanteilen in großen Insel-Verbundnetzen; PV-DIESEL-GLOBAL - Schlussbericht des Teilvorhabens „Simulation und verteilte Erzeugung“, https://doi.org/10.34657/28666, 2025.

Obradović, K., Dkhili, N., Sied, M. E., Réthoré, P.-E. M., and Das, K.: From the idea to construction: Aspects of relevance of the optimized physical design of renewable hybrid power plants, Sustainable Energy Technologies and Assessments, 78, 104 325, https://doi.org/https://doi.org/10.1016/j.seta.2025.104325, 2025.

O'Malley, M., Holttinen, H., Cutululis, N., Vrana, T. K., King, J., Gevorgian, V., Wang, X., Rajaei-Najafabadi, F., and Hadjileonidas, A.: Grand challenges of wind energy science – meeting the needs and services of the power system, Wind Energy Science, 9, 2087–2112, https://doi.org/10.5194/wes-9-2087-2024, 2024.

Pedersen, M. M., Forsting, A. M., van der Laan, P., Riva, R., Alcayaga Romàn, L. A., Criado Risco, J., Friis-Møller, M., Quick, J., Schøler Christiansen, J.-P., Valotta Rodrigues, R., Olsen, B. T., and Réthoré, P.-E.: PyWake 2.5.0: An open-source wind farm simulation tool, https://gitlab.windenergy.dtu.dk/TOPFARM/PyWake, publisher: DTU Wind, Technical University of Denmark, 2023.

https://doi.org/10.5194/wes-2026-218
Preprint. Discussion started: 24 November 2026
© Author(s) 2026. CC BY 4.0 License.



Penev, M., Bush, B., and Melaina, M.: H2FAST: Hydrogen Financial Analysis Scenario Tool [SWR 15-06], https://doi.org/10.11578/dc.20230522.1, 2019.

Peyghami, S., Davari, P., Fotuhi-Firuzabad, M., and Blaabjerg, F.: Standard Test Systems for Modern Power System Analysis: An Overview, IEEE Industrial Electronics Magazine, 13, 86–105, https://doi.org/10.1109/MIE.2019.2942376, 2019.

Souza de Alencar, M., Göçmen, T., and Cutululis, N. A.: Flexible cable routing framework for wind farm collection system optimization, European Journal of Operational Research, 329, 1037–1051, https://doi.org/https://doi.org/10.1016/j.ejor.2025.07.069, 2026.

Stanley, A. P. J. and Ning, A.: Massive simplification of the wind farm layout optimization problem, Wind Energy Science, 4, 663–676, https://doi.org/10.5194/wes-4-663-2019, 2019.

Svendsen, H. G., Vrana, T. K., Holdyk, A., and Schümann, H.: The Low Emission Oil and Gas Open reference platform—An off-grid energy system for renewable integration studies, IET Energy Systems Integration, 5, 66–79, https://doi.org/https://doi.org/10.1049/esi2.12085, 2023.

TESVOLT AG: Technisches Datenblatt TESVOLT TALLON, revision: b.01 edn., https://www.tesvolt.com/_media/02PRODUKTE/11_Tallon/TESVOLT_TALLON-Technisches_Datenblatt-DE.pdf, 2025.

Valencia Ochoa, G., Nunez Alvarez, J., and Acevedo, C.: Research Evolution on Renewable Energies Resources from 2007 to 2017: A Comparative Study on Solar, Geothermal, Wind and Biomass Energy, International Journal of Energy Economics and Policy, 9, 242–253, https://doi.org/10.32479/ijeep.8051, 2019.

Veers, P., Dykes, K., Basu, S., Bianchini, A., Clifton, A., Green, P., Holttinen, H., Kitzing, L., Kosovic, B., Lundquist, J. K., Meyers, J., O'Malley, M., Shaw, W. J., and Straw, B.: Grand Challenges: wind energy research needs for a global energy transition, Wind Energy Science, 7, 2491–2496, https://doi.org/10.5194/wes-7-2491-2022, 2022.

WindEurope: Renewable Hybrid Power Plants: Exploring the Benefits and Market Opportunities, Position Paper, available: https://windeurope.org/wp-content/uploads/files/policy/position-papers/WindEurope-renewable-hybrid-power-plants-benefits-and-market-opportunities.pdf, 2019.

Zahle, F., Barlas, A., Lønbæk, K., Bortolotti, P., Zalkind, D., Wang, L., Labuschagne, C., Sethuraman, L., and Barter, G.: Definition of the IEA Wind 22-Megawatt Offshore Reference Wind Turbine, Technical University of Denmark, https://doi.org/10.11581/DTU.00000317, dTU Wind Energy Report E-0243 IEA Wind TCP Task 55, 2024.

Zhang, Z., Ragonneau, T. M., and Schueller, J.: zaikunzhang/prima: Version 0.5, https://doi.org/10.5281/zenodo.8052655, 2023.

Zippenfenig, P.: Open-Meteo.com Weather API, https://doi.org/10.5281/zenodo.7970649, 2023.